



AN OPTIMISED PSEUDO-INVERSE ALGORITHM (OPIA) FOR MULTI-INPUT MULTI-OUTPUT MODAL PARAMETER IDENTIFICATION

FERMÍN. S. V. BAZÁN† AND CARLOS A. BAVASTRI‡

†*Departamento de Matemática–CFM*, ‡*Laboratório de Vibrações e Acústica*,
Universidade Federal de Santa Catarina, Florianópolis, SC Brazil

(Received July 1995, accepted November 1995)

A multi-input multi-output (MIMO) algorithm for modal parameter identification is developed based on linear prediction theory and its numerical efficiency compared to that of the well-known Eigensystem realisation algorithm ERA. The problem of determining the correct system's order is analysed through perturbation theory of singular values of oversized Hankel-block matrices. The popular technique of using overdetermined models to mitigate the effects of external noise on the quality of the estimated parameters is justified here by showing analytically that the system's singular values are enhanced when oversized Hankel matrices are used. Numerical experiments illustrating the performance of the proposed algorithm on both simulated and real mechanical systems, are included.

© 1996 Academic Press Limited

1. INTRODUCTION

Modal parameter identification is the procedure used to determine dynamic properties of vibrating systems from experimental data, such as damping, frequencies, mode shapes and modal participation factors, which are referred to as modal parameters. In recent years, several multiple-input multiple-output (MIMO) modal parameters identification methods have been specially developed to take advantage of the accuracy and consistency of the acquired data obtained by MIMO procedures. Such methods include the Ibrahim time domain [1, 2], the polyreference time and frequency domain method [1, 21, 23], the Eigensystem realisation algorithm in both the time and frequency domain [13, 14] and the direct parameter model method [15]. A common characteristic of those methods is their ability to improve the quality of the estimated parameters, as well as to handle closely spaced modes. In almost all these cases, the methods apply to data in processed form, either as frequency response functions FRFs, or the equivalents impulse response functions IRFs, typically found through the inverse Fourier transform. Several handicaps, however, still exist in MIMO modal parameter identification methods. One of the major problems is in the determination of the number of effective modes for a measured data set. It is widely known that in practical applications the use of overdetermined models is very useful to overcome this problem as well as to mitigate the effects of external noise. But, theoretical justifications explaining the benefits of using overdetermined models are rarely found. When this is the case, intuitive justifications are presented, see [22] for example. Another problem is how to distinguish between computational modes and actual modes of the structure to be identified.

The pseudo-inverse technique is a powerful tool for linear algebra that has found numerous applications in modal testing [7], and in a great variety of applied

sciences [2, 5, 6, 10, 19]. In particular, the modal parameter identification area has been widely favoured since, in general, pseudo-inverse matrices are used extensively during the development of methods for parameter identification. Even so, it is important to state that working with pseudo-inverse matrices is a delicate matter, mainly because elements of pseudo-inverse matrices are sensitive to small perturbations in the data, that is, small perturbations in the data can yield large perturbations in the computed pseudo-inverse. These facts are well-documented in numerical linear algebra [5, 9, 10, 18].

The purpose of this paper is to present a MIMO algorithm for modal parameter identification, giving the details of a time domain implementation and showing later that it can be implemented in the frequency domain. The algorithm, the optimised pseudo-inverse algorithm (OPIA), is based on linear prediction and makes use of super-dimensioned Hankel-block matrices, constructed with either sampled versions of the impulse response matrix function or the corresponding frequency response matrix function, which are estimated by using force and response signals measured simultaneously. The paper is organised as follows: section 2 is a tutorial, it includes the theory for MIMO modal parameter identification and certain basic results of linear algebra. Section 3 develops the proposed algorithm. Here, a rigorous singular value analysis of superdimensioned Hankel matrices is carried out in order to detect the system's correct order and also to explain why overdetermined models must be used for parameter identification. Finally, to illustrate the performance of the proposed algorithm, numerical experiments using both synthesised and real mechanical systems are included in Section 4.

2. MATHEMATICAL MODEL AND THEORY

2.1. MULTI-INPUT MULTI-OUTPUT RELATIONSHIPS

The theoretical basis of MIMO modal parameter identification methods is well documented in numerous sources [1, 7, 11]. A natural assumption is that the system under test is spatially discretised and that its dynamic behaviour is described by a set of differential equations of type

$$\mathbf{M}\ddot{\mathbf{u}} + \mathbf{C}\dot{\mathbf{u}} + \mathbf{K}\mathbf{u} = \mathbf{f}, \quad (1)$$

where \mathbf{M} , \mathbf{C} and \mathbf{K} are square matrices which represent the system's mass, damping and stiffness properties, respectively, \mathbf{u} is a vector of generalised co-ordinates representing displacement and \mathbf{f} the vector of excitation acting at each dof of the system. In practice, as dynamic signals are discrete in nature, due to truncation of the data in terms of frequency content and measurement errors, only a finite number of modes can be used to describe the dynamic behaviour of the system. Thus, if q excitations and p responses are available, a $p \times q$ impulse response function matrix $\mathbf{h}(t)$ may be found in order to describe the system's characteristics [1, 13, 22, 23]. The following relationship between impulse response functions and modal parameters can be established [1, 22]:

$$\mathbf{h}(t) = \mathbf{\Phi} e^{At}L, \quad (2)$$

where:

$$\mathbf{\Phi} = [\phi_1, \dots, \phi_n, \phi_1^*, \dots, \phi_n^*]_{p \times 2n}$$

is a mode shape matrix (vector ϕ_i is the i -th system's mode shape),

$$A = \text{diag}(\lambda_1, \dots, \lambda_n, \lambda_1^*, \dots, \lambda_n^*),$$

with the λ s being the system's eigenvalues, and;

$$L^T = [l_1, \dots, l_n, l_1^*, \dots, l_n^*]_{q \times 2n};$$

being the modal participation factor matrix, which indicates how well a particular input excites a particular mode. Here, the * symbol denotes complex conjugation and n the number of modes contained in the data. Parameters $\{\phi, \lambda_i, l_i\}$ are the so-called i th modal parameters of the system. Relation (2) can be expressed by:

$$\mathbf{h}(t) = \sum_{i=1}^n \phi_i l_i^T e^{\lambda_i t} + \phi_i^* l_i^{*T} e^{\lambda_i^* t} = \sum_{i=1}^n R_i e^{\lambda_i t} + R_i^* e^{\lambda_i^* t} \quad (3)$$

where the R s are the well-known residues matrices.

Frequency response matrices and impulse response matrices are related by $H(\omega) = \mathcal{F}[\mathbf{h}(t)]$, where \mathcal{F} denotes Fourier transformation. Hence

$$H(\omega_k) = \Phi A_k L, \quad (4)$$

where

$$A_k = \text{diag}\left(\frac{1}{j\omega_k - \lambda_1}, \dots, \frac{1}{j\omega_k - \lambda_n}, \dots, \frac{1}{j\omega_k - \lambda_1^*}, \dots, \frac{1}{j\omega_k - \lambda_n^*}\right), \quad j = \sqrt{-1}.$$

This paper deals with the development of algorithms for modal parameter identification, where equations (2) and (4) are extensively employed. The use of equation (2) is characteristic for the well-known time domain methods, while equation (4) is basic for frequency response approaches.

2.2. LINEAR ALGEBRA BACKGROUND

This section deals with the presentation of some basic results of linear algebra which are included for completeness. Given a matrix \mathbf{A} of order $M \times N$, there exists a unique matrix \mathbf{G} of the order $N \times M$ satisfying

$$(i) \mathbf{A}\mathbf{G}\mathbf{A} = \mathbf{A}, \quad (ii) \mathbf{G}\mathbf{A}\mathbf{G} = \mathbf{G}, \quad (iii) (\mathbf{A}\mathbf{G})^H = \mathbf{A}\mathbf{G}; \quad (iv) (\mathbf{G}\mathbf{A})^H = \mathbf{G}\mathbf{A}, \quad (5)$$

where superscript H denotes the transpose conjugate of a matrix. Matrix \mathbf{G} is the so-called pseudo-inverse matrix of \mathbf{A} and is denoted by $\mathbf{G} = \mathbf{A}^\dagger$. Conditions (i)–(iv) are known as the Moore–Penrose conditions. If \mathbf{A} is factored as $\mathbf{A} = \mathbf{B}\mathbf{C}$, such that \mathbf{B} is $M \times l$, \mathbf{C} is $l \times N$ and the rank of \mathbf{A} , \mathbf{B} and \mathbf{C} is l , then

$$\begin{aligned} (a) \mathbf{A}^\dagger &= \mathbf{C}^\dagger \mathbf{B}^\dagger, \\ (b) \mathbf{C}^\dagger &= \mathbf{C}^H (\mathbf{C}\mathbf{C}^H)^{-1}, \quad \text{and} \\ (c) \mathbf{B}^\dagger &= (\mathbf{B}^H \mathbf{B})^{-1} \mathbf{B}^H. \end{aligned} \quad (6)$$

Moreover,

$$\mathbf{B}^\dagger \mathbf{B} = \mathbf{I}_l = \mathbf{C}\mathbf{C}^\dagger, \quad (7)$$

where \mathbf{I}_l the $l \times l$ identity matrix. When \mathbf{A} is factored as above, it is said that this is a full-rank factorisation of \mathbf{A} . For the purpose of computing the pseudo-inverse of a matrix, relations expressed in (6) are fundamental [2]. Another important result is that related to the pseudo-inverse of a perturbed matrix. If $\tilde{\mathbf{A}} = \mathbf{A} + \mathbf{E}$, where \mathbf{E} is a matrix of small perturbations of \mathbf{A} , a question that arises is how close is $\tilde{\mathbf{A}}^\dagger$ to \mathbf{A}^\dagger ? An answer

to the question can be achieved through the singular value decomposition (SVD) of \mathbf{A} [5, 9]. This decomposition assures the existence of matrices, \mathbf{U} , \mathbf{V} and \mathbf{D} , such that

$$\mathbf{A} = \mathbf{U}\mathbf{D}\mathbf{V}^H, \quad (8)$$

where \mathbf{U} and \mathbf{V} are unitary matrices of order M and N respectively, and \mathbf{D} is the $M \times N$ matrix

$$\mathbf{D} = \begin{bmatrix} \sigma_1 & & & \\ & \sigma_2 & & \\ & & \ddots & \\ & & & \sigma_N \end{bmatrix}. \quad (9)$$

The σ s are the singular values of \mathbf{A} and satisfies

$$\sigma_1 \geq \sigma_2 \geq \dots \geq \sigma_N \geq 0. \quad (10)$$

Among other important information, the SVD of \mathbf{A} reveals that if $\text{rank}(\mathbf{A}) = l$, there are exactly l non-zero singular values and that the 2-norm of both \mathbf{A} and \mathbf{A}^\dagger are $\|\mathbf{A}\| = \sigma_1$ and $\|\mathbf{A}^\dagger\| = 1/\sigma_l$, respectively. By assuming the 2-norm as measure of closeness, if $\text{rank}(\tilde{\mathbf{A}}) = \text{rank}(\mathbf{A}) = l$, and $\|\mathbf{E}\| < \sigma_l$; then the following estimate holds [5, 10]

$$\frac{\|\mathbf{A}^\dagger - \tilde{\mathbf{A}}^\dagger\|}{\|\mathbf{A}^\dagger\|} \leq \frac{1 + \sqrt{5}}{2} \frac{k(\mathbf{A})}{1 - \frac{\|\mathbf{E}\|}{\sigma_l}} \frac{\|\mathbf{E}\|}{\|\mathbf{A}\|}. \quad (11)$$

Here, $k(\mathbf{A}) = \sigma_1/\sigma_l$, is the condition number of \mathbf{A} . The last relation says that to be $\tilde{\mathbf{A}}^\dagger \approx \mathbf{A}^\dagger$, in addition to the imposed conditions, $\|\mathbf{E}\|$ must be small when compared to σ_l , and \mathbf{A} must be well conditioned ($k(\mathbf{A}) = O(1)$), otherwise, the approximation of \mathbf{A}^\dagger by $\tilde{\mathbf{A}}^\dagger$ may be very poor. These results are well documented in numerical linear algebra [5, 9, 10, 18].

Another result is one that tells on the spectrum of the product of matrices. Let $\mathbf{A} \in \mathbb{C}^{M \times N}$ and $\mathbf{B} \in \mathbb{C}^{N \times M}$, $M \geq N$, where $\mathbb{C}^{M \times N}$ denotes the set of all complex $M \times N$ matrices. Then

$$\lambda(\mathbf{AB}) = \lambda(\mathbf{BA}) \cup \{0\}. \quad (12)$$

Here, $\lambda(\mathbf{A})$ denotes the spectrum of \mathbf{A} , a proof of this result can be seen in [18].

3. IDENTIFICATION PROCEDURE

The proposed algorithm is based on linear prediction [3, 4, 16, 17, 19]. In linear prediction one seeks a matrix containing the dynamic properties of the system and at the same time it predicts the future states of the system from the previous ones. The procedure used to develop OPIA is basically the same as that utilised in [4] for deriving the algorithms for parameter identification of single functions expressed as the sum of exponentials. This technique can be implemented in both the time and frequency domain.

3.1. PRELIMINARIES

The basic idea of time domain modal parameter identification methods is to form a numerical matrix, \mathbf{S} , whose eigenstructures reveals information about the modal parameters of the structure under test. Once the matrix \mathbf{S} is formed, the damping rates

and damped natural frequencies are found from the eigenvalues while the mode shapes are encountered from the corresponding eigenvectors. The matrix \mathbf{S} can be formed in different ways. In linear prediction, one forms a matrix equation

$$\mathbf{S}\mathbf{H}(j) = \mathbf{H}(j+1), \quad j = 0, 1, \dots \quad (13)$$

where $\mathbf{H}(j)$ are $(M \times p) \times (N \times q)$ Hankel-block matrices whose entries are samples of $\mathbf{h}(t)$: $\mathbf{h}_j = \mathbf{h}(j\Delta t)$, with Δt being the sampling interval

$$\mathbf{H}(j) = \begin{bmatrix} \mathbf{h}_j & \mathbf{h}_{j+1} & \cdots & \mathbf{h}_{j+N-1} \\ \mathbf{h}_{j+1} & \mathbf{h}_{j+2} & \cdots & \mathbf{h}_{j+N} \\ \vdots & \vdots & \ddots & \vdots \\ \mathbf{h}_{j+M-1} & \mathbf{h}_{j+M} & \cdots & \mathbf{h}_{j+M+N} \end{bmatrix}_{(M \times p) \times (N \times q)}$$

Next, for some j previously chosen, a matrix \mathbf{S} is calculated by pseudo-inversion:

$$\mathbf{S} = \mathbf{H}(j+1)\mathbf{H}(j)^\dagger. \quad (14)$$

It can be shown that the eigenstructure of \mathbf{S} so constructed contains the system's modal parameters. In fact, the Hankel matrix can be re-written as

$$\mathbf{H}(j) = \begin{bmatrix} \Phi \\ \Phi\bar{\Lambda} \\ \vdots \\ \Phi\bar{\Lambda}^{M-1} \end{bmatrix} \bar{\Lambda}[L \ \bar{\Lambda}L \ \cdots \ \bar{\Lambda}^{N-1}L] = \bar{\Phi}\bar{\Lambda}\bar{L}, \quad (15)$$

where $\bar{\Phi}$ and \bar{L} are easy to see in the context; and

$$\bar{\Lambda} = \text{diag}(e^{\lambda_1 \Delta t}, \dots, e^{\lambda_n \Delta t}, e^{\lambda_1^* \Delta t}, \dots, e^{\lambda_n^* \Delta t}). \quad (16)$$

If the system is controllable and observable [11, 14, 22], $\bar{\Phi}$ and \bar{L} are both of rank $2n$, and so $\text{rank}(\mathbf{H}(j)) = 2n, \forall j \geq 0$. Using equations (6) and (7),

$$\mathbf{H}(j+1)\mathbf{H}(j)^\dagger = \bar{\Phi}\bar{\Lambda}^{j+1}\bar{L}(\bar{\Phi}\bar{\Lambda}^j\bar{L})^\dagger = \bar{\Phi}\bar{\Lambda}^{j+1}\bar{L}\bar{L}^\dagger(\bar{\Lambda}^j)^\dagger\bar{\Phi}^\dagger = \bar{\Phi}\bar{\Lambda}\bar{\Phi}^\dagger,$$

which confirms the desired result. Moreover, using equation (6) and (7) again, one sees that

$$\mathbf{H}(j+1) = \bar{\Phi}\bar{\Lambda}^{j+1}\bar{L} = \bar{\Phi}\bar{\Lambda}\bar{\Phi}^\dagger\bar{\Phi}\bar{\Lambda}^j\bar{L} = \bar{\Phi}\bar{\Lambda}\bar{\Phi}^\dagger\mathbf{H}(j),$$

whence follows that $\bar{\Phi}\bar{\Lambda}\bar{\Phi}^\dagger$ is a matrix that performs as linear predictor and that the system's modal parameters can be extracted from its eigenstructure. Therefore, the matrix \mathbf{S} calculated by equation (14) performs as predictor as well as state matrix.

In practice, the system's order is not always known in advance and enough data must be taken to assure that M and N are both greater than $2n$. Moreover, it is known that the presence of noise in the data imposes the use of overdetermined models in order to minimise the distortion of the identified parameters as well as to detect the correct system's order [1, 3, 13, 14, 22]. In such cases, independently of the way how the pseudo-inverse is calculated, the size of the matrix \mathbf{S} becomes extremely large and considerable computational effort must be performed. For this reason, principle component analysis and minimal realisation approaches are suggested [1, 13, 14]. A typical algorithm that constructs a minimal realisation is ERA.

3.2. DERIVING OPIA IN THE TIME DOMAIN

For the purpose of deriving OPIA, first, observe that the Hankel matrices $\mathbf{H}(j+1)$ and $\mathbf{H}(j)$ can be related by

$$\mathbf{H}(j+1) = \mathbf{H}(j)\mathcal{C}, \quad \forall j \geq 0. \quad (17)$$

Here, \mathcal{C} is a $(N \times q) \times (N \times q)$ companion-block matrix defined by

$$\mathcal{C} = \begin{bmatrix} 0 & 0 & \cdots & 0 & c_1 \\ I_q & 0 & \cdots & 0 & c_2 \\ \vdots & \vdots & \vdots & \vdots & \vdots \\ 0 & 0 & \cdots & I_q & c_N \end{bmatrix}_{(N \times q) \times (N \times q)}, \quad (18)$$

with q being the number of columns of the entries in the Hankel-block matrices and the c_i s are $q \times q$ matrices, which must satisfy

$$\mathbf{H}(j)\hat{\mathcal{C}} = \hat{h}. \quad (19)$$

In this equation, $\hat{\mathbf{h}}$ and $\hat{\mathcal{C}}$ are both the last column vector-block of the matrices $\mathbf{H}(j+1)$ and \mathcal{C} respectively. Although equation (19) has infinite solutions, one always can impose unicity by computing the corresponding one of minimal norm.

Now, using the SVD theorem

$$\mathbf{H}(j) = \mathbf{U}\mathbf{D}\mathbf{V}^T = [\mathbf{U}_1 \mathbf{U}_2] \begin{bmatrix} \mathbf{D}_1 & 0 \\ 0 & \mathbf{D}_2 \end{bmatrix} \begin{bmatrix} \mathbf{V}_1^T \\ \mathbf{V}_2^T \end{bmatrix} = \mathbf{U}_1 \mathbf{D}_1 \mathbf{V}_1^T, \quad (20)$$

where, $\mathbf{U}_1, \mathbf{V}_1$ are matrices $(M \times p) \times 2n$ and $(N \times q) \times 2n$, respectively, and \mathbf{D}_1 is the $2n \times 2n$ diagonal matrix which contains the non-zero singular values of $\mathbf{H}(j)$. Observe that the above decomposition is a full-rank decomposition of $\mathbf{H}(j)$. Then, by using (6)–(a), it follows

$$\mathbf{H}(j)^\dagger = \mathbf{V}_1 \mathbf{D}_1^{-1} \mathbf{U}_1^T. \quad (21)$$

Using equations (21) and (20) in equation (14), by applying repeatedly the basic result expressed in equation (12), it follows that the spectrum of \mathbf{S} (discarding the zero eigenvalues) satisfies:

$$\lambda(\mathbf{S}) = \lambda(\mathbf{V}_1^T \mathcal{C} \mathbf{V}_1).$$

Therefore the system's eigenvalues can be extracted from the eigenvalues of

$$\bar{\mathbf{S}} = \mathbf{V}_1^T \mathcal{C} \mathbf{V}_1. \quad (22)$$

This relation constitutes the core of the current algorithm. Observe that the matrix $\bar{\mathbf{S}}$ is now $2n \times 2n$, i.e., it describes a reduced model of an order equal to the number of modes of the system.

The system's eigenmodes and the corresponding modal participation factors now need to be calculated. For this purpose, observe that \mathbf{S} [of (14)] and $\bar{\mathbf{S}}$ are related by

$$\mathbf{S} = \mathbf{U}_1 \mathbf{D}_1 \bar{\mathbf{S}} \mathbf{D}_1^{-1} \mathbf{U}_1^T. \quad (23)$$

If $\bar{\boldsymbol{\psi}}$ is an eigenvector matrix of $\bar{\mathbf{S}}$, from the above relation it follows that

$$\mathbf{S} \mathbf{U}_1 \mathbf{D}_1 \bar{\boldsymbol{\psi}} = \mathbf{U}_1 \mathbf{D}_1 \bar{\boldsymbol{\psi}} \bar{\boldsymbol{\lambda}}. \quad (24)$$

That is, $\mathbf{U}_1 \mathbf{D}_1 \bar{\boldsymbol{\psi}}$ is a matrix of eigenvectors of \mathbf{S} corresponding to the system's eigenvalues. Consequently, if E denotes the $p \times (M \times p)$ matrix defined by $E = [I_p \ 0]$, the system's

eigenmodes can be calculated by

$$\Phi = EU_1 D_1 \bar{\psi} \bar{\Lambda}. \quad (25)$$

Finally, once the system's eigenvalues and the mode shapes are calculated, the modal participation factors can be determined from equation (15) by a linear least square procedure. If \mathbf{F} is a $(N \times q) \times q$ matrix defined by $\mathbf{F} = [I_q \ 0]^T$, then

$$L = \bar{\Lambda}^{-j} \bar{\psi}^{-1} \mathbf{V}_1^T \mathbf{F}. \quad (26)$$

With the modal parameters at hand, single impulse responses can be synthesised by using (3). The proposed method (OPIA) suggests the estimation of modal parameters by using (22), (25) and (26).

Since both OPIA and ERA methods are derived using the SVD theorem, it seems appropriate to carry out a comparison regarding their numerical characteristics. ERA extracts the system's eigenvalues and mode shapes from the eigenstructure of a matrix, say, \mathbf{S}_E [13, 14], where

$$\mathbf{S}_E = \mathbf{D}_1^{-1/2} \mathbf{U}_1^T \mathbf{H}(j+1) \mathbf{V}_1 \mathbf{D}_1^{-1/2}. \quad (27)$$

It is easy to see that the work necessary for computing $\bar{\mathbf{S}}$ is equivalent to that used to form a product $\mathbf{V}_1^T \mathbf{V}_1$ plus a product of type $\mathbf{V}_1^T \mathcal{C}$, where \mathcal{C} comes from equation (19). When \mathcal{C} is of minimal norm, $\mathcal{C} = \mathbf{H}^*(j) \hat{\mathbf{h}} = \mathbf{V}_1 \mathbf{D}_1^{-1} \mathbf{U}_1^T \hat{\mathbf{h}}$, and so, $\mathbf{V}_1^T \mathcal{C} = \mathbf{D}_1^{-1} \mathbf{U}_1^T \hat{\mathbf{h}}$. Assuming \mathbf{D}_1 and \mathbf{V}_1 are available, $\mathbf{U}_1^T \hat{\mathbf{h}}$ can be easily calculated by means of equation (20) (without effective computation of \mathbf{U}_1). Thus, matrix $\bar{\mathbf{S}}$ can be formed efficiently using only the $2n$ -right singular vectors of $\mathbf{H}(j)$ and their corresponding singular values. But, since these singular vectors are eigenvectors of $\mathbf{A} = \mathbf{H}(j)^T \mathbf{H}(j)$, in a first attempt one could compute them through an eigendecomposition of \mathbf{A} . Indeed, this operation will be less expensive than performing a full SVD of $\mathbf{H}(j)$. One can verify, using MATLAB routines that, for example, forming matrix \mathbf{A} using a Hankel matrix 500×200 and performing its eigendecomposition, requires approximately a third of the time required for performing a full SVD of $\mathbf{H}(j)$. A disadvantage of forming \mathbf{A} is that, unless the product is formed in double-precision, numerical information can be lost due to rounded errors, and singular values will be calculated inaccurately. Fortunately, these effects do not perturb the largest eigenvalues and corresponding eigenvectors (this fact is widely known in computational linear algebra). It will be seen later that system's singular values are enhanced when oversized Hankel matrices are used. A less expensive procedure for computing estimates of \mathbf{V}_1 and \mathbf{D}_1 can be achieved from a partial eigendecomposition of \mathbf{A} . This can be reached using iterative methods, such as the block-power method (also called subspace iteration), or Lanczos method [20]. In applying these techniques, one must fix in advance a number p of desired eigenvectors. The number p must be a little bit larger than twice the anticipated number of system's modes. In practice, number p always can be estimated, for instance, by analysing a single FRF. In these conditions, it is obvious that, forming $\bar{\mathbf{S}}$ is much more economical than forming that one used by ERA. Although $\bar{\mathbf{S}}$, and \mathbf{S}_E are formed in a different way, extensive numerical computations have revealed that, (even with noise data), both OPIA and ERA yields modal parameters close to each other.

3.3. SINGULAR VALUE ANALYSIS, OVERDETERMINATION AND SYSTEM ORDER IDENTIFICATION

As was pointed out in subsection 3.1, the system's order can be identified from the rank of the matrices $\mathbf{H}(j)$. If noiseless data is used, the task is trivial, since the rank of $\mathbf{H}(j)$ can be identified by observing the $2n$ non-negligible singular values of this matrix. But, since in practice the available data are contaminated by external noise, a full-rank

Hankel matrix must be used: $\tilde{\mathbf{H}}(j) = \mathbf{H}(j) + \epsilon$, where ϵ represents a Hankel matrix of perturbations. This fact imposes an analysis of the conditions on the noise level in the data in order that one can be able to identify the system's order. For this purpose, let σ and $\tilde{\sigma}$ the singular values of $\mathbf{H}(j)$ and $\tilde{\mathbf{H}}(j)$ respectively. Using perturbation theory of singular values [5, 9, 18]:

$$\begin{cases} \tilde{\sigma}_i \leq \sigma_i + \|\epsilon\|, & i = 1, 2, \dots, 2n; \\ \tilde{\sigma}_i \leq \|\epsilon\|, & i = 2n + 1, n + 2, \dots, (N \times q). \end{cases} \quad (28)$$

From these inequalities one sees that if $\|\epsilon\|$ is small when compared to the $2n$ -th singular value of $\mathbf{H}(j)$, then there must exist a clear separation of the perturbed system's singular values: $\tilde{\sigma}_i, i = 1, 2, \dots, 2n$, from the noise singular values $\tilde{\sigma}_i, i = 2n + 1, n + 2, \dots, (N \times q)$. That is, if $\|\epsilon\| \ll \sigma_{2n}$, a set of singular values: $\{\tilde{\sigma}_1, \tilde{\sigma}_2, \dots, \tilde{\sigma}_{2n}\}$ must appear clearly enhanced, while in a second set, the perturbed singular values associated to the true zero singular values: $\{\tilde{\sigma}_{2n+1}, \tilde{\sigma}_{2n+2}, \dots, \tilde{\sigma}_{(N \times q)}\}$, must appear minimised, when compared to those of the first set. If one introduces a constant *Tol* defined by

$$Tol = \frac{1}{k(\mathbf{H}(j))} = \frac{\sigma_{2n}}{\sigma_1},$$

it is obvious that $\|\epsilon\| < \sigma_{2n}$ is equivalent to

$$0 < \frac{\|\epsilon\|}{\|\mathbf{H}(j)\|} < Tol \leq 1.$$

Constant *Tol* measures as a percentage a sort of *tolerance* for system order identification. If $\mathbf{H}(j)$ is well-conditional (σ_{2n} large) $Tol \approx 1$ and so the matrix signal to noise ratio: $\|\epsilon\|/\|\mathbf{H}(j)\|$ can be high. That is, well-conditioned Hankel matrices allow the identification of the system's order even for high noise level. When this is not the case, that is, when $\mathbf{H}(j)$ is ill-conditioned ($\sigma_{2n} \approx 0$), *Tol* is small and separation of system's singular values from noise singular values is impossible even for low signal to noise ratios.

The above analysis shows that the size of the $2n$ -th singular value of the Hankel matrix constructed with clean data plays an important role in the task of identifying the correct system's order. Consequently, estimates of σ_{2n} as a function of the dimension of $\mathbf{H}(j)$ must be calculated. In fact, from the full-rank decomposition of $\mathbf{H}(j)$ [see equation (15)], using (6a)

$$\|\mathbf{H}(j)^\dagger\| \leq \|\bar{L}^\dagger\| \|(\bar{A})^\dagger\| \|\bar{\Phi}^\dagger\|. \quad (29)$$

But this can be rewritten as

$$\sigma_{2n} \geq \frac{\beta^j}{\|\bar{\Phi}^\dagger\| \|\bar{L}^\dagger\|}, \quad \beta = \min\{|e^{i_j A t}|\}, \quad i = 1, 2, \dots, 2n. \quad (30)$$

This lower bound still can be written as a function of the modal parameters. Of course, this can be achieved by following closely a procedure like that one developed to prove Corollary 3.1 in [4] or by using variational properties of the Rayleigh quotient associated to $\bar{\Phi}^H \bar{\Phi}$ and $\bar{L}^H \bar{L}$ respectively. This done, one sees that

$$\|\bar{\Phi}^\dagger\| \leq \frac{\|\bar{\Phi}^\dagger\|}{\sqrt{1 + \beta^2 + \dots + \beta^{2M}}}, \quad \text{and} \quad \|\bar{L}^\dagger\| \leq \frac{\|\bar{L}^\dagger\|}{\sqrt{1 + \beta^2 + \dots + \beta^{2N}}}. \quad (31)$$

Inequality of the right side holds whenever $q \geq 2n$. Similar expressions can be derived for $q < 2n$. With these inequalities in equation (30), one could see that the following theorem holds.

THEOREM 3.1 If M and N are both larger than or equal to $2n$, then

$$\sigma_{2n} \geq \frac{\beta^j \sqrt{1 + \beta^2 + \cdots + \beta^{2M}} \sqrt{1 + \beta^2 + \cdots + \beta^{2N}}}{\|\Phi^\dagger\| \|L^\dagger\|}. \quad (32)$$

Observe that this lower bound depends on the dimension of $\mathbf{H}(j)$ and at the same time it increases as a function of M and N . The closer is the constant β to 1, the better the enhancing of σ_{2n} .

Summarising, the above analysis shows that when data noise are considered, overdetermined models must be used for identification due to two reasons: first, because the sufficient condition $\|\epsilon\| \ll \sigma_{2n}$ could be achieved; and second, because the conditioning of the Hankel matrix may be improved due to the enhancing of σ_{2n} (theoretical results which justify the decreasing of the condition number as a consequence of overdetermining the order of the model are still unknown and are the subject of research of the authors. The results of these investigations will be addressed in future work). It should be remembered that these conditions are important to have $\tilde{\mathbf{H}}(j)^\dagger \approx \mathbf{H}(j)^\dagger$. In such cases, the quality of the estimated parameters must be satisfactory. In working with experimental data, however, although σ_{2n} increase with the dimensions of the Hankel matrix, so do σ_1 and $\|\epsilon\|$. For this reason, it is clear that for severely noisy data, the rate of growth of σ_{2n} may not be as large as the rate of growth of $\|\epsilon\|$, and so a well-determined gap between $\tilde{\sigma}_{2n}$ and $\tilde{\sigma}_{2n+1}$ will not occur. These cases must be analysed by other methods. In practice, however, noise may be reduced by different means. This can be done for instance during the measurement process (by using averages) or by a judicious choice of the sequence of data to be analysed. This is useful, since some measurement data may be noisier than others. In these conditions, unless severe ill-conditioning is present, the condition $\sigma_{2n} \ll \|\epsilon\|$ should be satisfied as a consequence of using oversized data matrices. This point, as well as the improvement of the condition number of $k(\mathbf{H}(j))$, will be illustrated later using both simulated and experimental data. Another consequence of this analysis is that the behaviour of the lower bound for σ_{2n} [see equation (32)] provides information that can be utilised to determine an effective level of overdetermination not larger than necessary. For instance, if one supposes $\beta = 0.98$ and $M = N = 100$, then $\beta^{2M} \approx 0.01$, hence, successive overdetermination levels using M and N larger than 100 will not improve the referred lower bound (for overdamped systems constant β may be much less than 0.98).

Remarks

1. The singular value analysis of $\mathbf{H}(j)$ is important mainly from the theoretical point of view, since in practical applications, M and N may be extremely large and performing a full-SVD could be expensive. In these cases, it is sufficient to compute a partial SVD consisting of the p largest singular values and the corresponding singular vectors only. A suggestion is to calculate a partial SVD for a truncating level consisting of twice the number of peaks identified in some plot describing a mean Fourier spectrum of some column of $\mathbf{h}(t)$. Algorithms to compute a partial SVD can be found in [20]. Another possibility is to replace the full-SVD by a RRQR factorisation. It is well-known that this factorisation is able to detect the numerical rank of a matrix saving substantially computational effort [6].

2. Analogous to ERA, OPIA has a counterpart in the frequency domain. For the purpose of deriving OPIA in the frequency domain, complex Hankel-like block matrices whose entries are shift versions of the frequency response matrix, must be used. Once these matrices are formed, the same procedure as displayed in the time domain can be followed. Details on how these matrices areas formed can be found in [14].
3. A useful procedure to estimate better the effective rank of $\mathbf{H}(j)$ can be carried out by defining the *relative gap* g_i [10], between the singular values $\tilde{\sigma}_i$ and $\tilde{\sigma}_{i+1}$ by $g_i = \tilde{\sigma}_i/\tilde{\sigma}_{i+1}$. The number of effective modes can be revealed when there exists a well-determined gap for some i . This can be seen in a plotting of the gap g_i as function of i . A well-determined gap will not occur either because ill-conditioning is present or because the level of overdetermination is not large enough to dominate the amount of noise in the data.

Proposed algorithm (OPIA):

- Step 1. For $j \geq 0$ and $p \geq 2n$, compute the p -right singular vectors corresponding to the p -largest singular values of $\tilde{\mathbf{H}}(j)$. This done, estimate the order of the system.
- Step 2. Construct $\tilde{\mathbf{S}}$ according to (22).
- Step 3. Compute an eigenstructure of $\tilde{\mathbf{S}}$: $\{\bar{\mathbf{A}}, \bar{\boldsymbol{\psi}}\}$.
- Step 4. Use information from the previous steps and compute the system's eigenmodes and modal participation factor matrix according to equations (25) and (26) respectively.

4. SOME EXPERIMENTS WITH OPIA

To illustrate the performance of the proposed algorithm, simulation studies with known vibrating systems and experimental data analysis were carried out. The numerical simulations are referred to identification problems for simulated mechanical systems of 3 and 2 dof, respectively, employing data with and without noise. The theoretical singular value analysis developed in Section 3.3 is illustrated here in a quantitative manner. A practical application is addressed to identify the modal parameters of a building structure. The data set for this was acquired in the Laboratory of Vibration and Acoustics of the Federal University of Santa Catarina, SC, Brazil.

4.1. NUMERICAL SIMULATIONS

Example 1: Single IRF of a three dof mechanical system

In order to corroborate the pertinency of developing a singular value analysis of Hankel matrices constructed with clean data, a single signal defined by

$$h(t) = e^{-0.06t} \text{sen}(4t) + 0.8 e^{-0.056t} \text{sen}(7t) + 1.2 e^{-0.09t} \text{sen}(9t),$$

TABLE 1
Tol and σ_6 as function of the order of $\mathbf{H}(0)$

Singular value analysis		
Order	<i>Tol</i> (%)	σ_6
6	1.8787e-05	1.1461e-04
20	48.37	4.8100
40	64.21	11.7920

TABLE 2
Results of OPIA Analysis—example 1

k	True parameters		Estimated parameters	
	r_k	λ_k	\hat{r}_k	$\hat{\lambda}_k$
1	0.500i	-0.060-4.00i	0.003 + 0.490i	-0.0956-3.988i
2	0.400i	-0.056-7.00i	-0.002 + 0.387i	-0.0550-7.006i
3	0.600i	-0.090-9.00i	-0.001 + 0.601i	-0.0875-8.992i

was utilised. For this, Hankel matrices whose entries are sample of $h(t)$ recorded at a rate of $\Delta t = 0.1$ s were analysed. As the underlying signal corresponds to a 3 d.o.f. system, $\text{rank}(\mathbf{H}(j)) = 6, \forall j \geq 0$, a singular value analysis directioned to observe the behaviour of σ_1 and σ_6 , for Hankel matrices of various orders, was carried out. Results are shown in Table 1. As consequence of this analysis, oversized Hankel matrices were very well-conditioned; therefore changes for system’s order identification were excellent even for high levels of noise. This fact is attributed to the surprising enhancing of σ_6 as function of the order. The OPIA analysis was performed using a Henkel matrix of order 40×40 whose entries were perturbed by random noise in various levels. The noise level was measured by the ratio $\|noise\|/\|signal\|$. In this case, system’s order identification was not difficult because in terms of tolerance the constant Tol is high when compared to the noise level in the data. In these cases, modal parameter identification is a simple task. Results are presented for the case in which data with noise level of 30% was employed, see Table 2.

Example 2. Synthesized two dof mechanical system (SIMO-Scheme)

In order to discuss a case in which system’s order identification is difficult, an analytical mechanical system having high damping rates was analysed. For this, assume a system described by

$$\begin{bmatrix} 1 & 0 \\ 0 & 1 \end{bmatrix} \begin{bmatrix} \ddot{u}_1 \\ \ddot{u}_2 \end{bmatrix} + \begin{bmatrix} 2 & 0 \\ 0 & 8 \end{bmatrix} \begin{bmatrix} \dot{u}_1 \\ \dot{u}_2 \end{bmatrix} + \begin{bmatrix} 22 & -10\sqrt{2} \\ -10\sqrt{2} & 40 \end{bmatrix} \begin{bmatrix} u_1 \\ u_2 \end{bmatrix} = \begin{bmatrix} f_1 \\ f_2 \end{bmatrix}$$

The experiment started by calculating the first column of the impulse response matrix associated to the system: $[h_{11}(t) \ h_{21}(t)]^T$. Next, with the purpose of simulating a modal test using as data base IRFs corresponding to a single input and six outputs, ‘new’ IRFs were constructed by taking arbitrary linear combinations of $h_{11}(t)$ and $h_{21}(t)$. Thus, a modal test was simulated by applying the current algorithm for identifying the modal parameters using samples of a 6×1 impulse response matrix: $\mathbf{h}(t) = [h_{11}(t) \ h_{21}(t) \ \dots \ h_{61}(t)]^T$. The next

TABLE 3
 Tol and σ_4 as a function of the order of $\mathbf{H}(0)$

Singular value analysis		
Order	Tol (%)	σ_4
6×60	4.01e-07	4.50e-09
18×60	0.8532	0.0164
36×60	1.3553	0.0346
48×60	1.4824	0.0416

TABLE 4
Results of OPIA analysis—example 2

k	True parameters	Estimated parameters
	λ_k	$\hat{\lambda}_k$
1	$-3.00 + 5.00i$	$-2.56 + 5.65i$
2	$-2.00 + 4.00i$	$-1.19 + 3.47i$

task was to analyse the behaviour of the fourth singular value of the oversized Hankel matrix in order to know the tolerance for system's order identification. For this purpose IRFs were sampled using $\Delta t = 0.05$. It was verified that $\mathbf{h}_j \approx 0$, from $j \geq 100$, therefore the level of overdetermination of the model was limited by the number of available samples. Behaviour of σ_4 and tolerances for the system's order identification are shown in Table 3. Analogous to the first example, a surprising growing of constant Tol can be observed again; even so the oversized Hankel matrix constructed with the available data do not allow the identification of the system's order in the presence of noise, since Tol is very small. These facts can be explained by observing that the system under analysis have a mean damping rate $\xi \approx 0.48$, this implies that the constant β defined in equation (30) is not large enough to allow an effective increase of the lower bound of σ_4 . Results of OPIA analysis, employing data corrupted by random noise with level of 1.5% and a Hankel matrix of order 40×60 are shown in Table 4. The behaviour of σ_4 and Tol justifies the poor obtained results.

4.2. ANALYSING EXPERIMENTAL DATA: (BUILDING STRUCTURE)

As an example of an application of the OPIA method to a real system, a building structure has been chosen. The structure under test corresponds to a prototype of the three stages of industrial building. All results to be presented were obtained from two sets of impulse response functions which describes the input–output relationships between 20 input locations from point 11 until point 30 and a single output point located in point 29, see Fig. 1. The first data set corresponds to lateral excitation in the global x -direction while the second set corresponds to excitation in the global z -direction. In order to estimate the impulse response functions, first the corresponding FRFs were calculated. Each FRF relative at each pair of input–output points was obtained as result of averaging 15 FRFs related to these points obtained previously via an impact test procedure. Signal responses were filtered with a cut-off frequency of 200 Hz and measured with a single accelerometer

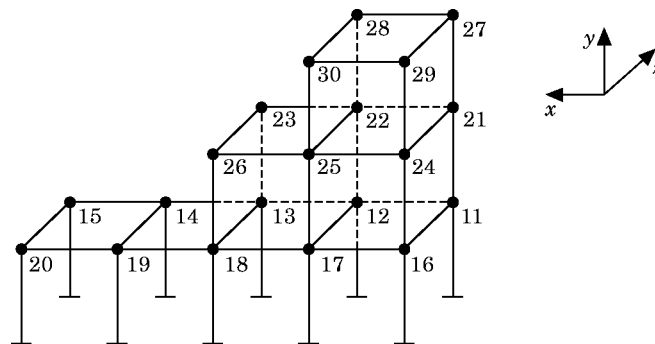


Figure 1. Prototype of industrial building structure.

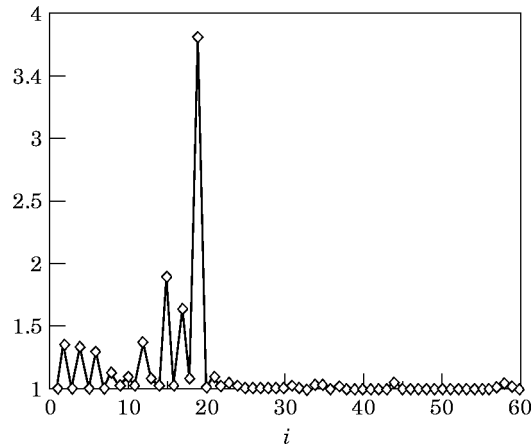


Figure 2. Trend of relative gap. \diamond , g_i .

for each data set. Dynamic signals were recorded during 8 s at a rate of 512 samples per second. All of the 40 impulse response functions were employed for modal identification in two distinct numerical experiments using data related to x and z directions, respectively, arranging the data corresponding to each direction in a single column of the impulse response matrix: $\mathbf{h} = [h_{11}(t) \ h_{21}(t) \ \dots \ h_{201}(t)]^T$.

The OPIA analysis was carried out in a PC environment using only 512 samples beginning from $j = 10$. The system order was identified analysing the behaviour of the relative gap and the mean Fourier spectrum of the data. This can be seen in Figs 2 and 3, which show the behaviour of the 60 first relative gap's corresponding to a Hankel block matrix of the first experience, constructed with 50 row-blocks and 200 columns, and the mean Fourier spectrum of all the data, respectively. In order to evaluate the performance of OPIA, the FRFs corresponding to the full frequency domain data were sent to ICATS (Imperial College Analysis Testing and Software), a modal analyser

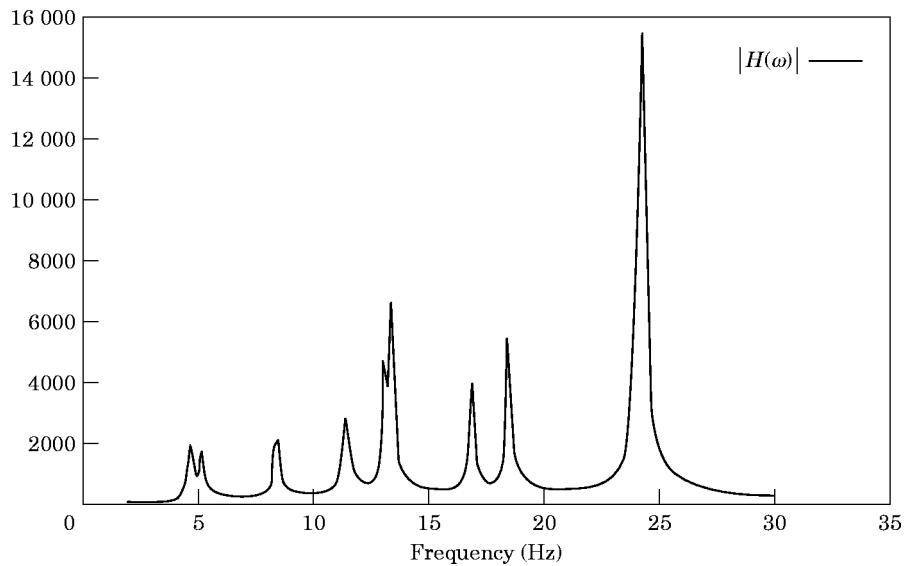


Figure 3. Mean Fourier spectrum.

TABLE 5
A comparison of results: OPIA vs. ICATS (first experiment)

Mode	ICATS		OPIA	
	Damping ξ (%)	Frequency ω (Hz)	Damping ξ (%)	Frequency ω (Hz)
1	0.83	4.75	0.79	4.75
2	0.91	5.16	0.96	5.17
3	0.51	8.47	0.53	8.47
4	0.32	11.49	0.31	11.49
5	0.29	13.10	0.31	13.11
6	0.31	13.37	0.30	13.37
7	0.29	16.93	0.29	16.94
8	0.19	18.52	0.18	18.53
9	0.15	24.28	0.14	24.28

software, and a global modal parameter identification was requested. Results obtained by both OPIA and ICATS are shown in Tables 5 and 6 respectively. These tables show that natural frequencies and damping rates identified by OPIA are remarkably close to those calculated using ICATS, except that, in the last case, the second mode was not identified, perhaps because of the short length of the data sequence utilised, due to the limitations of working in a PC environment. Even so, the results obtained were sufficient to illustrate a good performance of OPIA.

To strengthen the theory developed in subsection 3.3, the impulse response functions corresponding to the input–output relationships in the x direction were synthesised [this was done by using parameters of Table 5 and relation (3)]. With the impulse response functions at hand, ‘errorless’ Hankel-block data matrices $\mathbf{H}(j)$ of several orders were constructed. This done, the corresponding error matrices ϵ , were computed simply making $\epsilon = \tilde{\mathbf{H}}(j) - \mathbf{H}(j)$, where $\tilde{\mathbf{H}}(j)$ were the Hankel matrices constructed with experimental data. Next, a singular value analysis of these matrices was carried out. The experiment was designed to observe the size of both $\tilde{\sigma}_{18}$ and σ_{18} , as well as the size of the error $\|\epsilon\|$, for successive orders of overdetermination. This was done by maintaining the number of fixed columns and varying the number of row blocks. An analogous experiment was

TABLE 6
A comparison of results: OPIA vs. ICATS (second experiment)

Mode	ICATS		OPIA	
	Damping ξ (%)	Frequency ω (Hz)	Damping ξ (%)	Frequency ω (Hz)
1	0.83	4.75	0.82	4.81
2	0.91	5.16	—	—
3	0.51	8.47	0.52	8.48
4	0.32	11.49	0.37	11.48
5	0.29	13.10	0.38	13.11
6	0.31	13.37	0.31	13.38
7	0.29	16.93	0.33	16.94
8	0.19	18.52	0.18	18.53
9	0.15	24.28	0.22	24.23

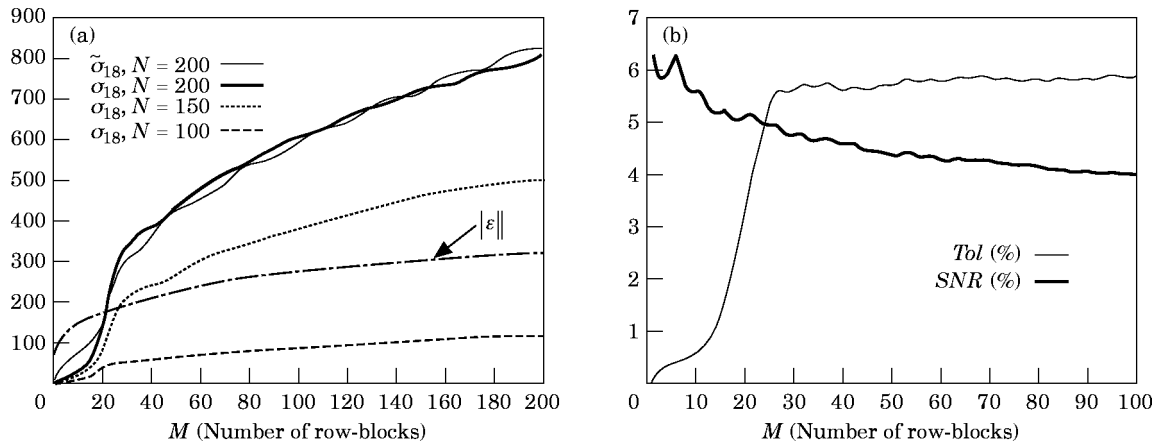


Figure 4. σ_{18} vs. $\|\epsilon\|$ and Tol vs. SNR ($N = 200$).

carried out for observing the behaviour of constants Tol and SNR both defined in Section 3.3. Results of these experiments are shown in Fig. 4. By observing these figures, the positive effects of overdetermining the order of the model becomes evident, since both, σ_{18} and the tolerance to the system's order identification (Tol) are both enhanced, as predicted in theory. Observe that both M and N must be suitably chosen, otherwise, the amount of noise in the data need not be dominated by the size of σ_{2n} , as can be seen in Fig. 4(a) for the case $N = 100$. Empirical results have pointed out that σ_{2n} is better enhanced when $M = N$, however this must be demonstrated analytically.

5. CONCLUSIONS

An optimised pseudo-inverse algorithm (OPIA) for parameter identification in the linear prediction context has been presented and its performance illustrated with numerical experiments analysing simulated data as well as data corresponding to a real structure. It is shown via the SVD theorem and suitable manipulation that it is possible to improve the well-known ERA method, preserving efficiency as well as diminishing computational effort. The problem of detecting the number of effective modes was tackled using *relative gaps*, taking advantage of the singular value analysis of Hankel-block matrices specially developed for this situation. This analysis also became useful to explain the benefits of the use of overdetermined models in parameter identification.

ACKNOWLEDGMENT

This work was supported in part by CNPQ grant 300487/94-O(NV).

REFERENCES

1. R. J. ALLEMANG and D. L. BROWN 1987 Final Report, Department of Mechanical and Industrial Engineering, University of Cincinnati. *Experimental Analysis and Dynamic Component Synthesis*, Vol. III—*Modal Parameter Estimation*.
2. J. BAUMEISTER 1987 Stable Solution of Inverse Problems, G. Fisher (ed.). Braunschweig.
3. F. S. V. BAZÁN 1993 Doctoral Thesis, Department of Mechanical Project, FEM/UNICAMP, Campinas, SP, Brazil. *Desenvolvimento de Técnicas de Identificação Paramétrica em Sistemas Mecânicos no Domínio do Tempo*.

4. F. S. V. BAZÁN and L. H. BEZERRA 1994 Technical Report, Department of Mathematics, Federal University of Santa Catarina. *Singular Value Analysis in Parameter Identification Problems (to appear in the Proceedings of XVIII CNMAC Curitiba PR, Brazil)*.
5. A. BJORK 1990 Least squares problems. In *Handbook of Numerical Analysis*, Vol. 1 *Solution of Equations in \mathbb{R}^n* . Amsterdam: Elsevier North Holland.
6. T. F. CHAN and P. C. HANSEN 1992 *SIAM Journal of Scientific Statistics in Computing* **13**, 215–224. Some applications of the rank revealing QR-Factorization.
7. D. J. EWINS 1984 *Modal Testing and Practice*. John Wiley & Sons Inc, New York.
8. J. A. FABUNMI 1986 *AIAA Journal* **24**, 504–509. Effects of structural modes on vibratory force determination by the pseudo-inverse technique.
9. G. H. Golub and C. F. Van Loan 1989 *Matrix Computations*. Baltimore MD: The Johns Hopkins University Press.
10. P. C. HANSEN 1987 *BIT* **27** 534–553. The truncated SVD as a method for regularization.
11. D. J. INMAN 1989 *Vibration with Control Measurements and Stability*. Englewoods Cliffs, NJ: Prentice Hall.
12. S. R. IBRAHIM and E. C. MIKULCIK 1977 *Shock and Vibration Bulletin* **47**(4). A method for the direct identification of vibration parameters from the free response.
13. JER-JAN JUANG and R. S. PAPPÀ 1985 *Journal of Guidance, Control and Dynamics* **8**, 620–627. An eigensystem realization algorithm for modal parameter identification and model reduction.
14. JER-JAN JUANG 1987 *Journal of Modal Analysis* **1**, 1–18, Mathematical correlation of modal parameter identification methods via system realization theory.
15. J. LEURIDAN *et al.* *ASME Paper* 85-DET-90. Time domain parameter identification methods for linear modal analysis: a unifying approach.
16. Z. LIANG and D. J. INMAN 1990 *Journal of Vibrations and Acoustics* **112**, 410–413. Matrix decomposition methods in experimental modal analysis.
17. J. MAKHOUL 1975 *Proceedings of the IEEE* **63**(4). Linear prediction: a tutorial review.
18. G. W. STEWART and Ji-GUANG SUN 1990 *Matrix Perturbation Theory*, and perturbation of pseudo-inverses. Boston, MA: Academic Press.
19. B. D. RAO 1988 *IEEE Transaction Acoustics Speech and Signal Processing ASSP* **36**, Perturbation analysis of an SVD-based linear prediction method for estimating the frequencies of multiple sinusoids.
20. C. R. VOGEL and J. G. WADE 1994 *SIAM Journal of Scientific Computing* **15**, 736–754. Iterative SVD-based methods for ill-posed problems.
21. H. VOLD and T. ROCKLIN 1982 *Proceedings of the International Modal Analysis Conference*, pp. 542–548. The numerical implementation of a multi-input modal estimation algorithm for mini-computers.
22. Q. J. YANG *et al.* 1994 *Mechanical Systems and Signal Processing* **8**, 159–174. A system theory approach to multi-input multi-output modal parameters identification method.
23. L. ZHANG AND H. KANDA 1988 *Shock and Vibration Bulletin*, pp. 11–17. The algorithm and application of a new multi-input-multi-output modal parameter identification method.